GEOPHYSICAL RESEARCH LETTERS, VOL. 35, L20103, doi:10.1029/2008GL035433, 2008

Observations of molecular oxygen ions in Saturn's inner magnetosphere

Hilary R. Martens,[1] Daniel B. Reisenfeld,[1] John D. Williams,[1] Robert E. Johnson,[2] and H. Todd Smith[3]

Received 22 July 2008; revised 2 September 2008; accepted 12 September 2008; published 21 October 2008.

[1] We present an analysis of molecular oxygen ion (O_2^+) abundance in Saturn's inner magnetosphere based on observations made with the Cassini Plasma Spectrometer (CAPS). Using data summed over 23 orbits, we resolve and isolate O_2^+ counts from the tail of the water group ion mass distribution (W^+ [O^+, OH^+, H_2O^+, H_3O^+]) and from background sources. O_2^+ was initially estimated at ~1–2% of the total ion population in the inner magnetosphere based on CAPS data from the Saturn orbital insertion pass. Through refined analysis techniques, we have found O_2^+ to account for just above 0.3% of all W^+ ions at L = 4.5, with only minor fluctuations in relative density out to L = 7.5 – 8.0. Beyond L = 7.5, the relative O_2^+/W^+ abundance exhibits a statistically significant increase through L = 10.5, which may indicate a neutral O_2 source in the vicinity of Rhea.
Citation: Martens, H. R., D. B. Reisenfeld, J. D. Williams, R. E. Johnson, and H. T. Smith (2008), Observations of molecular oxygen ions in Saturn's inner magnetosphere, *Geophys. Res. Lett.*, *35*, L20103, doi:10.1029/2008GL035433.

1. Introduction

[2] The Cassini spacecraft has been orbiting Saturn for over four years, returning far more data than the Pioneer and twin Voyager spacecraft combined, in an unprecedented mission to study the planet, its satellites, and its magnetosphere. Cassini's long-term, direct observation of Saturn's plasma environment has allowed a rigorous investigation into magnetospheric composition, including the presence and source of minor ion populations (i.e., <5% of the total ion population). Analysis of these minor species can provide clues to the origin and evolution of Saturn's rings and satellites. Here we focus our investigation on molecular oxygen ions (O_2^+) in Saturn's inner magnetosphere (L-shell$\leq$11).

[3] Prior to Cassini, laboratory experiments and Hubble Space Telescope observations suggested the presence of water products in Saturn's magnetosphere [e.g., *Johnson et al.*, 1989; *Shemansky et al.*, 1993; *Jurac et al.*, 2002], and ozone (O_3) in the icy surfaces of Dione and Rhea [*Noll et al.*, 1997]. During Saturn Orbital Insertion (SOI), Cassini detected an ionosphere dominated by O_2^+ and O^+ over Saturn's main rings [*Tokar et al.*, 2005; *Young et al.*, 2005; *Waite et al.*, 2005]. *Johnson et al.* [2006] determined that these ions are photo-ionization products of neutral O_2, which is produced primarily through photo-induced decomposition of ring particles into H_2 and O_2. Radiation-induced decomposition can also occur via high-energy charged-particle impacts on ice grains in the tenuous rings and icy satellite surfaces [*Johnson et al.*, 2006]. Due to the relatively small gravity of Saturn's satellites and rings, the decomposed ice particles form toroidal oxygen atmospheres as observed above the main rings [*Johnson et al.*, 2006; *Tokar et al.*, 2005] and as predicted at the icy satellites [e.g., *Sittler et al.*, 2004] and tenuous E, F, and G rings.

[4] Using Cassini Ion Mass Spectrometer (IMS) data collected during SOI, *Sittler et al.* [2005] estimated the O_2^+ abundance in Saturn's inner magnetosphere ($4 \leq L \leq 14$) at roughly 1–2% of the total ion population. *Johnson et al.* [2005] described how the O_2 from the rings may attain relatively large energies and be redistributed throughout the magnetosphere before becoming ionized. The question of whether detections of O_2^+ outside the main rings indicate additional local sources of O_2 remains open.

[5] In this paper we present an analysis of O_2^+ abundances in Saturn's inner magnetosphere using Cassini Plasma Spectrometer (CAPS) IMS data collected over 23 orbits of the Cassini spacecraft. We consider whether the O_2^+ distribution suggests additional sources of O_2. Due to the relative weakness of the O_2^+ signal, special attention must be paid to the method by which quantitative information is extracted. Thus, we first describe in detail the analysis technique, followed by a discussion of our results.

2. Data Collection

[6] The CAPS IMS consists of a top-hat style electrostatic analyzer, followed by a linear electric field time-of-flight (TOF) mass analyzer. TOF spectra are collected as a function of analyzer voltage, yielding two-dimensional energy-versus-TOF arrays. (See *Young et al.* [2004] for details on IMS operation.) Mass analysis is facilitated by two detector systems: the high-resolution ($M/\Delta M \sim 60$) linear electric field (LEF) detector and the lower resolution ($M/\Delta M \sim 8$) straight-through (ST) detector. Despite lower mass resolution, the ST detector boasts higher detection efficiencies than the LEF detector, which is useful for amplifying the weak signals from minor magnetospheric constituents. Hence, data obtained by the ST detector are used exclusively in our investigation.

[7] TOF spectra for 23 orbits between the dates of 27 October 2004 and 27 March 2006 were first summed and then binned by distance from Saturn for every 0.5 dipole L-shell interval from L = 3.5 to L = 14. Periapses of

[1]Department of Physics and Astronomy, University of Montana, Missoula, Montana, USA.
[2]Department of Engineering Physics, University of Virginia, Charlottesville, Virginia, USA.
[3]JHU APL, Laurel, Maryland, USA.

0094-8276/08/2008GL035433$05.00

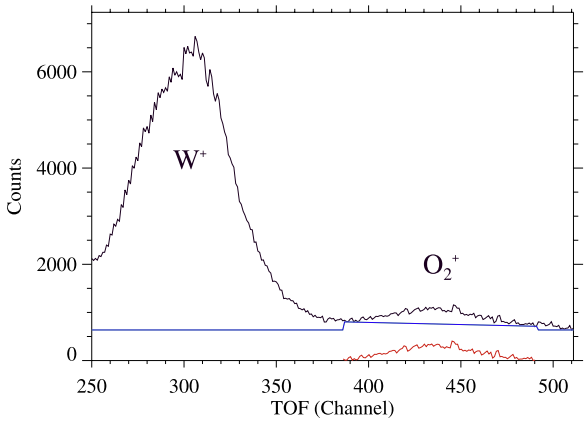

Figure 1. Time-of-flight spectrogram for L = 5.5 − 6.0 at energy 666.4 eV, zoomed in to focus on the O_2^+ peak. The black line indicates the original counts prior to background subtraction. The blue indicates the background subtraction. The red line depicts the difference between the black and blue lines and represents the final set of counts to be applied to our O_2^+ summation method.

these orbits fall within the dusk-side portion of the magnetosphere, generally between 16 and 20 local time. Although these orbits span ±22° of latitude, over half of them were equatorial.

[8] By summing large amounts of data we can amplify a weak O_2^+ signal over a significant background radiation signal and/or overlap with the spectral tails of the dominant ion population, the water group ions (O^+, OH^+, H_2O^+, and H_3O^+; or collectively, W^+). This allows us to detect and quantify O_2^+ abundances from L = 4.5 to L = 11. Although we also detect O_2^+ inward to L = 3.5, penetrating radiation overwhelms the O_2^+ signal for L < 4.5, significantly reducing our detection confidence for this region and preventing useful analysis. Likewise, O_2^+ is qualitatively observed outward to at least L = 12; however, beyond L = 11, the signal weakens significantly and soon drops below the detection limits of the IMS.

[9] Inward of the plasmasphere boundary at L ∼ 14, we expect the plasma to be nearly co-rotating [*Young et al.*, 2005; *Sittler et al.*, 2006; *Wilson et al.*, 2008], but, as CAPS is not always directed toward the co-rotational plasma flow, data filtration was necessary to minimize the effect of plasma anisotropy on the composition analysis. Hence, we removed data obtained when the direction of co-rotation was 30° beyond the CAPS field of view as well as when CAPS was not actuating. (The CAPS actuator rotates the IMS aperture through 220° to compensate for CAPS being mounted on a non-spinning spacecraft.) Also, to avoid contaminating the dataset with composition conditions localized to a particular satellite's environment, all satellite encounters are explicitly excluded.

3. Species Isolation

[10] To determine W^+ abundance, we used an automated analysis method whereby model peaks derived from IMS calibration were fit to the TOF spectra via a linear least-squares algorithm. Dependable for dominant ion populations, this method has been routinely applied to the analysis of IMS composition data [*Young et al.*, 2005; *Tokar et al.*, 2005; *Sittler et al.*, 2006]. However, the procedure becomes less reliable when dealing with minor ion populations because, although the model functions accurately fit the central portion of peaks, uncertainties become significant in the far tails due to differences in the calibration and space environments. Hence, when subtracting the model function for a major species (e.g., H_2O^+) to reveal the presence of a minor species (e.g., O_2^+) that appears in the tail, the potential exists to miscount the content of the minor species, requiring the use of an alternative isolation method.

[11] Hence, for a given L-shell bin of our summed TOF spectra, O_2^+ was isolated using a multi-step process to remove background and W^+ tail counts. First, a flat background correction eliminated the majority of background counts. Next, TOF spectra for certain energies, typically between ∼400–2000 eV, required the subtraction of a sloped baseline to account for the W^+ tail, which could not be accurately determined by the automated fitting method previously described. In such cases, the boundaries of the O_2^+ peak were determined by empirically fitting the mass peaks and finding intersection points between the W^+ and O_2^+ peak tails. Next, the minima within 10 channels on either side of both O_2^+ boundary points were determined; one standard deviation of the count values was added to avoid underestimating the W^+ tail contamination (i.e., to determine the average, not minimum, background); and the resultant line connecting the two points was subtracted from the isolated O_2^+ peak. Figure 1 depicts this process graphically for the summed TOF spectra between L = 5.5 − 6.0.

[12] Figure 2 is an example of the summed TOF spectrogram for L = 5.5 − 6.0, restricted to a TOF range of 250–511 channels, and an energy range of 41.6–21,300 eV. The spectrogram, plotted after the removal of background counts, illustrates the prominent W^+ population as well as the region selected for O_2^+ count integration, depicted by the red box. Despite the relative weakness of the O_2^+ signal, it is well resolved from W^+ because O_2^+ peaks at energies a

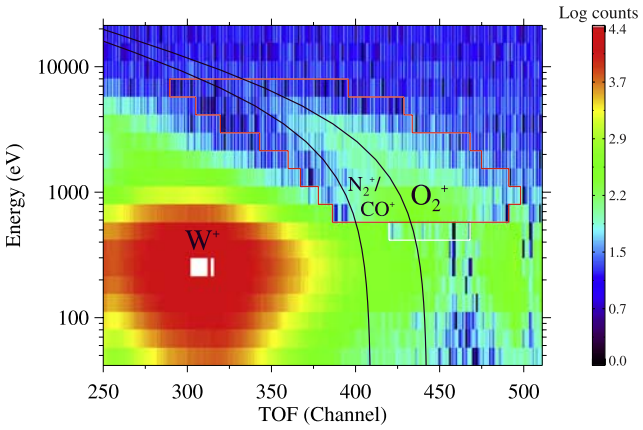

Figure 2. Time-of-flight spectrogram depicting the summation of counts over the analysis period for L = 5.5 − 6.0. The curved, black lines indicate the calculated peak centers for (left) N_2^+/CO^+ and (right) O_2^+. The red box indicates the determined boundaries for the O_2^+ peak. The white box extension represents a more uncertain O_2^+ detection, included as a source of error.

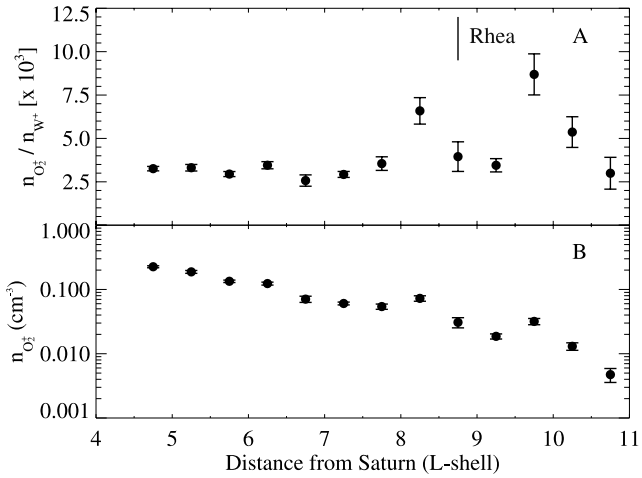

Figure 3. O_2^+ number densities: (a) Density ratio of O_2^+ to W^+ as a function of L-shell distance from Saturn. Error is quoted at the 1-σ level. (b) Absolute O_2^+ densities determined by scaling our O_2^+/W^+ density ratio by *Wilson et al.*'s [2008] parameterized fit to W^+.

factor of 2–3 higher than W^+. However, the O_2^+ count contribution does become difficult to resolve at lower energies where the W^+ counts peak (white-bounded extension in Figure 2). The uncertainty from isolating counts at these energies dominates the error estimate for O_2^+ abundance. Additional sources of uncertainty arise from counting statistics and uncertainty in the detection efficiency. Note that because each radial bin is composed of counts summed over multiple orbits, the error bars reflect an uncertainty in the mean and not variability in the environment.

[13] *Smith et al.* [2008] have reported the presence of a small mass-28 population in Saturn's inner magnetosphere as well (i.e., N_2^+ and/or CO^+), contained within the left shoulder of the O_2^+ peak. The mass-28 population is difficult to quantify, however, due to limited mass resolution and its proximity to O_2^+. Fitting calibration-determined model functions to the data reveals an average $(N_2^+ + CO^+)/O_2^+$ relative abundance of ~2% over the investigation region (consistent with the rough upper limits placed on N_2^+/CO^+ by *Smith et al.* [2008]). However, because of the large uncertainty in the fitting procedure and the small size of the contribution, we have chosen not to correct the O_2^+ abundance for the mass-28 contribution, but do include it as a source of uncertainty.

4. Results and Discussion

[14] Figure 3a presents our calculated O_2^+/W^+ relative number densities as a function of distance from Saturn. The mass of the collective W^+ distribution was approximated at 17 amu. Figure 3b depicts an estimate of absolute O_2^+ number density, calculated by scaling the O_2^+/W^+ ratio by a parameterized fit to the equatorial water group density ($n_{W^+} = 162.1 \exp(-0.042L^2)$, as reported by *Wilson et al.* [2008].

[15] Our analysis indicates that, on average, O_2^+ number density is just above 0.3% relative to W^+ at L = 4.5, with only minor fluctuations out to L = 7.5 – 8.0. Since O_2^+ and W^+ are close in mass, the relatively flat density ratio for L = 4.5 – 7.5 is consistent with sources for both species being primarily interior to L = 4.5 (i.e., the rings for O_2^+ [*Tokar et al.*, 2005] and Enceladus for W^+ [*Tokar et al.*, 2006]). Beyond L = 7.5, however, the relative density ratio increases. For L = 4.5 – 7.5, the average relative density ratio is 0.31 ± 0.01%; for L = 7.5 – 10.5, it is 0.41 ± 0.02%. Thus, the increase in O_2^+ abundance beyond L = 7.5 is statistically significant, suggesting the possibility of additional O_2^+ sources or a change in the ionization and/or loss rate. Additional sources might include local E-ring grains and, since Rhea orbits at ~8.75R_S, the surface of Rhea and its newly inferred ring particles [*Jones et al.*, 2008].

[16] The energetic protons and electrons present in Saturn's magnetosphere are relatively inefficient sputtering agents, but cause the decomposition of icy surfaces into O_2 and H_2 [*Johnson*, 1996; *Johnson and Quickenden*, 1997], contributing to the neutral population in Saturn's magnetosphere [*Sittler et al.*, 2004]. Since the density of ice grains in Saturn's E-ring increases inward of Rhea's orbit [*Showalter et al.*, 1991], and the density of energetic protons decreases rapidly inside of ~8R_S [*Paranicas et al.*, 2008], an enhancement in the region seen in Figure 3a is possible due to decomposition of E-ring grains. However, the total surface area of the E-ring at this orbital region is orders of magnitude smaller than the surface area of Rhea, Saturn's largest icy satellite. In addition, the energetic electron population (~10's of keV) exhibits strong depletions at Rhea's orbit and over a region on the order of a few Rhea radii [*Jones et al.*, 2008], suggesting that energetic charged particles are depositing energy into Rhea's surface and its ring. Presuming Rhea's surrounding material is primarily icy, like Rhea's surface, the energy deposited will be a source of O_2. The decomposition of ice by particle radiation is corroborated by earlier observations of O_3 trapped in Rhea's surface ice [*Noll et al.*, 1997]. Therefore, we suggest this additional source of O_2 produces our observed enhancement in relative O_2^+ abundance.

[17] We estimated a rough source rate for O_2 production from Rhea and its putative trapped ice grains using the observed depletions in energetic electron flux [*Jones et al.*, 2008]. Due to the considerable uncertainty in O_2 production efficiency, the source rate should be considered an order-of-magnitude estimate. Ejected molecules are tracked in Saturn's gravitational field until they are lost by ionization or charge exchange [e.g., *Johnson et al.*, 2004; *Sittler et al.*, 2008]. Figure 4 compares the local O_2 column density to the column of O_2 that has been scattered out of Saturn's ring atmosphere [*Johnson et al.*, 2006]. Although both are order-of-magnitude estimates, an enhancement in O_2 density, implying a relative increase in O_2^+, is consistent with a Rhea source. In addition, the spatial extent of the enhancement in the O_2 column density is consistent with the ion data. The simulated neutral column densities, however, are well below the upper limits established by MIMI ENA and UVIS observations [*Jones et al.*, 2008], and therefore could only be detected as a source of plasma ions.

[18] Although this enhancement is roughly consistent with our observations, it does not show the apparent drop in O_2^+ relative abundance at Rhea's orbit, as seen in Figure 3a. Since the enhancement in O_2^+ is locally produced, whereas W^+ is primarily a product of outward diffusion at this orbital radius [*Sittler et al.*, 2008], the drop may be due to the large target presented by Rhea's gravitationally bound

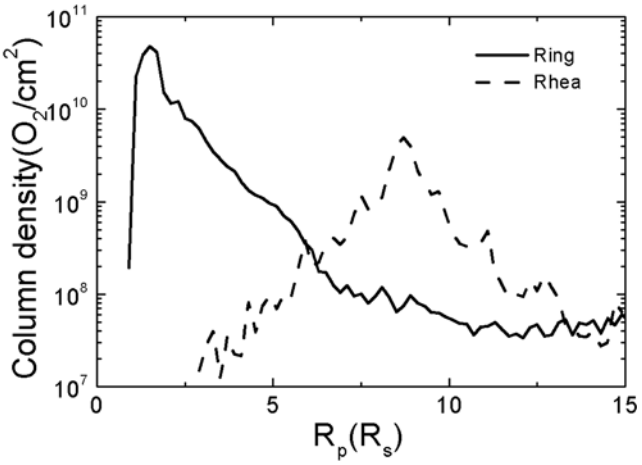

Figure 4. Simulations of the O_2 neutral column density as a function of radial distance from Saturn (1 Saturn radii [R_S] = 60330 km). Solid line: O_2 scattered from over the main rings by ion-molecule collisions [*Johnson et al.*, 2006]: source rate (S) $\sim 4 \times 10^{26}$ O_2/s; loss is through re-impacting main rings; ejecta speed distribution is due to ion-neutral scattering; over the main rings the total column of O_2 is the scattered component shown here plus the unscattered component ($\sim 10^{13}$ O_2/cm^2/s [*Johnson et al.*, 2006]). Dashed line: O_2 from Rhea and its ring material, assumed to be water ice. S is estimated from energy deposited by energetic particles [*Jones et al.*, 2008] and lifetime, τ, is taken from *Sittler et al.* [2008]: $S\tau \sim 2 \times 10^{31}$ particles. These sources are order-of-magnitude estimates. Although the source rate from the vicinity of Rhea is 2–3 orders of magnitude smaller, the ejected O_2 survive about 3 orders of magnitude longer since those ejected from the rings have a very high probability of re-impact in one orbit.

grains to the fresh pick-up ions. That is, the gravitationally bound grains preferentially absorb O_2^+ ions, which have very large gyro radii, at a faster rate than the outward diffusing W^+ ions.

5. Summary and Conclusions

[19] Using CAPS IMS data, we have analyzed molecular oxygen ion abundance in Saturn's inner magnetosphere. On average, O_2^+ number density is just above 0.3% relative to W^+ at L = 4.5, with only minor fluctuations out to L = 7.5. This marks the transition to a statistically significant increase in relative density out to L = 11, which may indicate that Rhea and its putative ring are sources of neutral O_2, and hence O_2^+, in the inner magnetosphere. Although the observed enhancement here could be consistent with a local increase in the ionization rate or a radial variation in the proton flux, we suggest that the enhancement is consistent with recent observations that indicate large depletions in energetic electrons within Rhea's Hill sphere. Such energetic particles are a source of O_2 by radiation-induced decomposition of icy materials. It also appears that O_2^+ produced throughout the toroidal cloud are being absorbed preferentially by Rhea and its cloud of ice grains, accounting for the apparent drop in O_2^+/W^+ relative density between L = 8.5 and L = 9.5.

[20] **Acknowledgments.** This work was supported by JPL contract 1243218 for CAPS operations and data analysis.

References

Johnson, R. E. (1996), Sputtering of ices in the outer solar system, *Rev. Mod. Phys.*, *68*, 305–312.

Johnson, R. E., and T. I. Quickenden (1997), Photolysis and radiolysis of water ice on outer solar system bodies, *J. Geophys. Res.*, *102*, 10,985–10,996.

Johnson, R. E., M. K. Pospieszalska, E. C. Sittler, A. F. Cheng, L. J. Lanzerotti, and E. M. Sieveka (1989), The neutral cloud and heavy ion inner torus at Saturn, *Icarus*, *77*, 311–329.

Johnson, R. E., R. W. Carlson, J. F. Cooper, C. Paranicas, M. H. Moore, and M. C. Wong (2004), Radiation effects on the surface of the Galilean satellites, in *Jupiter: The Planet, Satellites and Magnetosphere*, edited by F. Bagenal et al., pp. 485–512, Cambridge Univ. Press, Cambridge, U.K.

Johnson, R. E., M. Liu, and E. C. Sittler Jr. (2005), Plasma-induced clearing and redistribution of material embedded in planetary magnetospheres, *Geophys. Res. Lett.*, *32*, L24201, doi:10.1029/2005GL024275.

Johnson, R. E., et al. (2006), Production, ionization and redistribution of O_2 in Saturn's ring atmosphere, *Icarus*, *180*, 393–402.

Jones, G. H., et al. (2008), The dust halo of Saturn's largest icy moon, Rhea, *Science*, *319*, 1380–1384.

Jurac, S., M. A. McGrath, R. E. Johnson, J. D. Richardson, V. M. Vasyliunas, and A. Eviatar (2002), Saturn: Search for a missing water source, *Geophys. Res. Lett.*, *29*(24), 2172, doi:10.1029/2002GL015855.

Noll, K. S., T. L. Roush, D. P. Cruikshank, R. E. Johnson, and Y. J. Pendleton (1997), Detection of ozone on Saturn's satellites Rhea and Dione, *Nature*, *388*, 45–47.

Paranicas, C., et al. (2008), Sources and losses of energetic protons in Saturn's magnetosphere, *Icarus*, *197*, 519–525.

Shemansky, D. E., P. Matheson, D. T. Hall, H.-Y. Hu, and T. M. Tripp (1993), Detection of the hydroxyl radical in the Saturn magnetosphere, *Nature*, *363*, 329–332.

Showalter, M. R., J. N. Cuzzi, and S. M. Larson (1991), Structure and particle properties of Saturn's E ring, *Icarus*, *94*, 451–473.

Sittler, E. C., R. E. Johnson, S. Jurac, J. D. Richardson, M. McGrath, F. Crary, D. T. Young, and J. E. Nordholt (2004), Pickup ions at Dione and Enceladus: Cassini Plasma Spectrometer simulations, *J. Geophys. Res.*, *109*, A01214, doi:10.1029/2002JA009647.

Sittler, E. C., et al. (2005), Preliminary results on Saturn's inner plasmasphere as observed by Cassini: Comparison with Voyager, *Geophys. Res. Lett.*, *32*, L14S07, doi:10.1029/2005GL022653.

Sittler, E. C., et al. (2006), Cassini observations of Saturn's inner plasmasphere: Saturn orbit insertion results, *Planet. Space Sci.*, *54*, 1197–1210.

Sittler, E. C., et al. (2008), Ion and neutral sources and sinks within Saturn's inner magnetosphere: Cassini result, *Planet. Space Sci.*, *56*, 3–18.

Smith, H. T., M. Shappirio, R. Johnson, D. B. Reisenfeld, E. Sittler, F. J. Crary, D. J. McComas, and D. Young (2008), Enceladus: A potential source of ammonia products and molecular nitrogen for Saturn's magnetosphere, *J. Geophys. Res.*, doi:10.1029/2008JA013352, in press.

Tokar, R. L., et al. (2005), Cassini observations of the thermal plasma in the vicinity of Saturn's main rings and the F and G rings, *Geophys. Res. Lett.*, *32*, L14S04, doi:10.1029/2005GL022690.

Tokar, R. L., et al. (2006), The interaction of the atmosphere of Enceladus with Saturn's plasma, *Science*, *311*, 1409–1412.

Waite, J. H., Jr., et al. (2005), Cassini Ion and Neutral Mass Spectrometer measurements of oxygen ions near Saturn's A-ring, *Science*, *307*, 1260–1262, doi:10.1126/science.1105734.

Wilson, R. J., R. L. Tokar, M. G. Henderson, T. W. Hill, M. F. Thomsen, and D. H. Pontius Jr. (2008), Cassini Plasma Spectrometer thermal ion measurements in Saturn's inner magnetosphere, *J. Geophys. Res.*, doi:10.1029/2008JA013486, in press.

Young, D. T., et al. (2004), Cassini Plasma Spectrometer investigation, *Space Sci. Rev.*, *114*, 1–112.

Young, D. T., et al. (2005), Composition and dynamics of plasma in Saturn's magnetosphere, *Science*, *307*, 1262–1264.

R. E. Johnson, Department of Engineering Physics, University of Virginia, Thornton Hall, Charlottesville, VA 22903, USA.

H. R. Martens, D. B. Reisenfeld, and J. D. Williams, Physics and Astronomy, University of Montana, 32 Campus Drive, Number 1080, Missoula, MT 59812, USA. (hilarymartens@gmail.com)

H. T. Smith, JHU APL, 11100 Johns Hopkins Road, MP3-E175, Laurel, MD 20723, USA.